PARTICLE FILTERING METHODS FOR MOTION ANALYSIS IN TAGGED MRI

Ihor Smal, Wiro Niessen, Erik Meijering

Biomedical Imaging Group Rotterdam,
Departments of Medical Informatics and Radiology
Erasmus MC – University Medical Center Rotterdam, The Netherlands
Email: i.smal@erasmusmc.nl

ABSTRACT

Myocardial tagging using magnetic resonance imaging (MRI) is a well-known noninvasive method for studying regional heart dynamics. While it offers great potential for quantitative analysis of a variety of kinematic and kinetic parameters, its clinical use has so far been limited, mainly due to mediocre performance of existing tag tracking algorithms under poor imaging conditions. In this paper we propose a new approach to tracking of MRI tag intersections. It is based on a Bayesian estimation framework, implemented by means of particle filtering, and combines information about heart dynamics, the imaging process, and tag appearance. Since at any time point it optimally incorporates all available information, it can be expected to be more robust and accurate. This is demonstrated by results of preliminary experiments on image sequences from (small) animal imaging studies.

Index Terms— Particle filtering, tracking, tagged MRI.

1. INTRODUCTION

During the last decades, myocardial tissue tagging with magnetic resonance imaging (MRI) has shown great potential for noninvasive measurement of the motion of a beating heart. In cardiac imaging, the major task is the analysis of cardiac motion for identification of ischemic and infarcted tissues. Contrary to methods that require implantation of radiopaque beads or ultrasonic crystals, using spatial modulation of magnetization (SPAMM) [1] enables noninvasive measurement of material displacement and deformation of myocardium by tagging regions of the heart wall and following their motion in subsequent images. With SPAMM, two orthogonal sets of magnetic saturation planes, each orthogonal to the image plane, can be created in short time (see Fig. 1), where the intersection of the stripes provides two-dimensional information about the displacement of material points.

The process of identifying and tracking tag intersections manually, to analyze the relative motion of tags and calculate local strain and rotation, is time consuming and laborious. Existing automatic techniques [2–7] are usually based on segmentation/detection of tags separately in every frame using variations of active contour models and are not robust enough to deal with varying quality of typical experimental image data. The alternative automatic technique based on harmonic phase magnetic resonance imaging (HARP) [8] uses isolated spectral peaks in the Fourier domain of MR tagged images and analyzes the complex phase images, which can be treated as material property and related to myocardial strain. With these techniques, reliable tag tracking can mostly be achieved only in the first few frames of the image sequence.

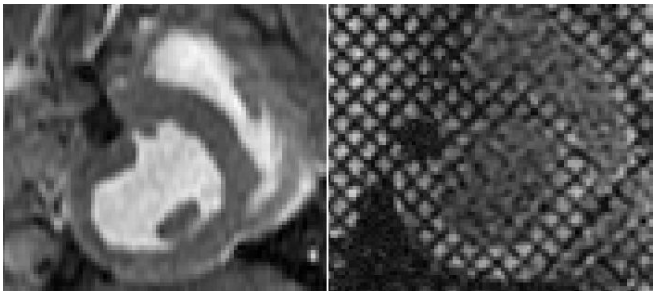


Fig. 1. Examples of images from studies of pig hearts: untagged (left) and tagged (right) MR images, single short-axis slices (Courtesy T. Springeling, Erasmus MC).

In this paper we propose a new particle filtering (PF) based method for analysis of tagged MRI data. It is built within a Bayesian estimation framework and combines the information about the heart dynamics, the imaging process, and tag appearance in tracking the tagging pattern. Additionally, the information from all available images at any time point is utilized, which improves the robustness and performance of the proposed technique. The results of tag tracking are used to reconstruct dense motion and strain fields.

2. METHOD

In the application under consideration, the main task is to track the tag lines or line intersections (see Fig. 1) to ob-

Financial support by the European Commission (FP7-grant 201842).

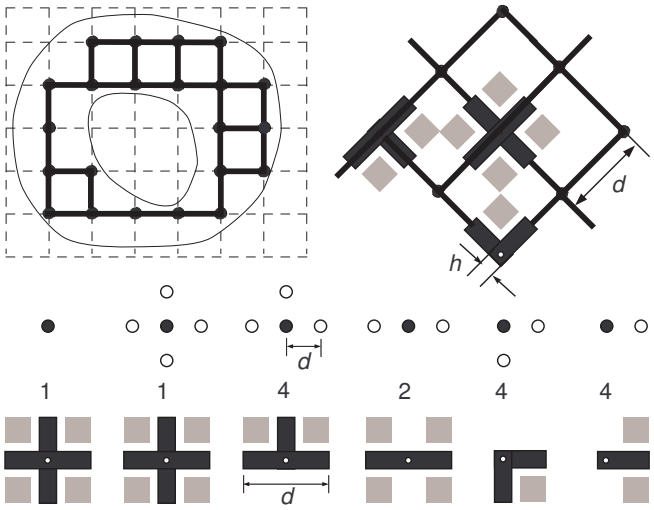


Fig. 2. Top row: example of initialization, where two LV contours define the bounding box and a set of line intersections that are used for tracking (left) and positioning of the observation models depending on the neighborhood (right, $\theta_T = 45°$). Bottom row: the possible neighborhood configurations and corresponding observation models with indicated number of possible unique rotations.

tain the displacement field that describes myocardial behavior during a heart cycle. Using the displacement information, other relevant measures such as local strain and torsion can be readily computed and used in practice for classification of (ab)normal heart function. Commonly, the analysis of tagged MR images consists of three steps [2–7]. First, the endocardial and epicardial contours of the left ventricle (LV) are defined either manually or with semi-automated algorithms [5]. Second, the tag lines are segmented in every image of the sequence. In most cases, the line intercessions are used as feature points during the tracking. Third, the tag line positions are used to fit either parametrized model of cardiac displacement [2] or reconstruct a dense displacement field [9] from sparse measurements using interpolation techniques such as thin-plate splines [10] or B-spline solids [3, 7].

We propose to replace the second step with a novel PF-based method capable of robust and accurate tracking of tag line intersections even in cases of poor image quality, which is inherent in this application due to the fading of tagging in time. Additionally, such replacement simplifies the first step of the framework because it eliminates the necessity to define the LV contours in every frame of the image sequence, which is also a nontrivial and error-prone task. In our case, the LV contours are defined only in the first frame, where two orthogonal sets of tag lines represent a non-deformed grid and have the highest contrast. Here, the tag lines are automatically detected within a rectangular region of interest that bounds the epicardial contour (Fig. 2) by pattern (grid) matching, as the distance between the lines d, the line thickness h and the grid orientation θ_T are known from the acquisition protocol. The line intersections between two LV contours (hereafter called "tags") are further tracked using the proposed method. Each tag has at most 4 neighbors and all 16 possible neighborhood configurations are shown in Fig. 2. The coordinates and the neighborhood type k_m ($k = \{1, \ldots, 16\}$) of each tag m, together with the parameters d, h, and θ_T are used for initialization of the proposed method.

Bayesian Tag Tracking. Within the Bayesian estimation framework, we aim to estimate the tag locations in time taking into account the noisy measurements (MR image sequence) and prior knowledge about the system (heart) dynamics. At each time step t, the tag is described by a state vector $\mathbf{s}_t = (x_t, y_t, \theta_t)$, where (x_t, y_t) and θ_t define the spatial position and local orientation, respectively. In this case, the Bayesian tracking approach is used to recursively estimate a time evolving posterior distribution (so called filtering distribution) $p(\mathbf{s}_t|\mathbf{z}_{1:t})$ that describes the tag state $\mathbf{s}_t$ given all the observations $\mathbf{z}_{1:t} = \{\mathbf{z}_1, \ldots, \mathbf{z}_t\}$ up to time t. The exact solution to this problem can be constructed by specifying the Markovian probabilistic model of the state evolution $D(\mathbf{s}_t|\mathbf{s}_{t-1})$ and the likelihood $L(\mathbf{z}_t|\mathbf{s}_t)$ that relates the noisy measurements to any possible state $\mathbf{s}_t$. The required probability density function (pdf) $p(\mathbf{s}_t|\mathbf{z}_{1:t})$ may be obtained, recursively, in two steps: prediction and update [11, 12]

$$p(\mathbf{s}_t|\mathbf{z}_{1:t-1}) = \int D(\mathbf{s}_t|\mathbf{s}_{t-1}) p(\mathbf{s}_{t-1}|\mathbf{z}_{1:t-1}) d\mathbf{s}_{t-1}, \quad (1)$$

$$p(\mathbf{s}_t|\mathbf{z}_{1:t}) \propto L(\mathbf{z}_t|\mathbf{s}_t) p(\mathbf{s}_t|\mathbf{z}_{1:t-1}). \quad (2)$$

In our case, the initial pdf is given in terms of a Dirac delta function, $p(\mathbf{s}_0|\mathbf{z}_0) = \delta(\mathbf{s}_0 - \hat{\mathbf{s}}_0)$, where for each tag at time $t = 0$, the initial position $\hat{\mathbf{s}}_0 = (\hat{x}_0, \hat{y}_0, \theta_T)$ is known from the initialization procedure described above. The filtering distribution embodies all available statistical information and an optimal estimate of the state such as expectation, maximum a posteriori (MAP), or minimum mean square error (MMSE) estimates, may be obtained from the pdf [11, 12].

The straightforward generalization of the Bayesian formulation to the problem of multi-tag tracking, where the determination of the multimodal posterior distribution over the joint configuration of the tags is required, is computationally prohibitive due to the increase in dimensionality of the state space [11, 12]. Similar to our previous work on tracking in microscopy [13], in order to capture the multi-modal nature and avoid computational problems, the filtering distribution can be modeled as an M-component mixture [14],

$$p(\mathbf{s}_t|\mathbf{z}_{1:t}) = \textstyle\sum_{m=1}^{M} \pi_{m,t} p_m(\mathbf{s}_t|\mathbf{z}_{1:t}) \quad (3)$$

with $\sum_{m=1}^{M} \pi_{m,t} = 1$ and non-parametric models for the individual mixture components (the filtering distributions for each of M tags). In this case, the dimensionality of the state space does not change and (3) can be updated in the same fashion as the two-step approach for standard Bayesian sequential estimation [14].

The optimal Bayesian solutions defined by the recurrence relations (1) and (2) are analytically tractable only in a restrictive set of cases [11]. For most practical models of interest,

sequential Monte Carlo methods [11, 12] (also known as particle filtering (PF)) are used as an efficient numerical approximation. Here, the required posterior $p_m(\mathbf{s}_t|\mathbf{z}_{1:t})$ for each tag m is represented as a set of N_s random samples ("particles") and associated normalized weights $\{\mathbf{s}_{m,t}^{(i)}, w_{m,t}^{(i)}\}_{i=1}^{N_s}$ as $p_m(\mathbf{s}_t|\mathbf{z}_{1:t}) \approx \sum_{i=1}^{N_s} w_{m,t}^{(i)} \delta(\mathbf{s}_t - \mathbf{s}_{m,t}^{(i)})$, and the filtering distribution (3) is approximated by $\{\{\mathbf{s}_{m,t}^{(i)}, w_{m,t}^{(i)}\}_{i=1}^{N_s}\}_{m=1}^{M}$. The solution using PF is given by a recursive procedure that predicts the state from time $t-1$ to t and updates the weights based on newly arrived measurements $\mathbf{z}_t$ as

$$\mathbf{s}_{m,t}^{(i)} \sim D(\mathbf{s}_{m,t}|\mathbf{s}_{m,t-1}^{(i)}) \text{ and } w_{m,t}^{(i)} \propto w_{m,t-1}^{(i)} L(\mathbf{z}_t|\mathbf{s}_{m,t}^{(i)}), \tag{4}$$

$i = 1, \ldots, N_s$, $m = 1, \ldots, M$. At each time step, the tag position is estimated from $p_m(\mathbf{s}_t|\mathbf{z}_{1:t})$ using the MMSE estimator. In order to apply the described framework in practice, two models, $D(\mathbf{s}_t|\mathbf{s}_{t-1})$ and $L(\mathbf{z}_t|\mathbf{s}_t)$, have to be specified, which we describe next.

Observation Model. For each tag m, the likelihood $L(\mathbf{z}_t|\mathbf{s}_t)$ of the state $\mathbf{s}_{m,t}$ is dependent on the location of that tag within the grid (the neighborhood) and is given by one of the 16 models depicted in Fig. 2. The observation model for the state $\mathbf{s}_{m,t}$ is positioned at $(x_{m,t}, y_{m,t})$ in the image and with the orientation $\theta_{m,t}$. The type of the model is defined by k_m, which is computed during the initialization (at time $t = 0$) by examining the configuration of the grid. The average image intensities in the "black" and "gray" rectangular regions are computed (μ_0 and μ_1, respectively) and the difference is used to define the likelihood as

$$L(\mathbf{z}_t|\mathbf{s}_{m,t}, k_m) = \begin{cases} \exp\left(\frac{\mu_1 - \mu_0}{\gamma}\right) - 1, & \mu_1 - \mu_0 > 0, \\ 0, & \mu_1 - \mu_0 \leq 0, \end{cases} \tag{5}$$

where the scaling factor γ controls the sensitivity (peakness) of the likelihood. The parameters that characterize the gray and black regions in the observation model (d and h, see Fig. 2) are known from the acquisition settings.

Dynamical Model. The state evolution is specified by the prior $D(\mathbf{s}_t|\mathbf{s}_{t-1})$, which in our case is modeled as a constrained random walk. The sampling of the new states (see (4)) is done according to

$$\mathbf{s}_{m,t}^{(i)} = \mathbf{s}_{m,0}^{(i)} + a(\mathbf{s}_{m,t-1}^{(i)} - \mathbf{s}_{m,0}^{(i)}) + \mathbf{u}_t, \tag{6}$$

where $0 \leq a \leq 1$ controls if the new states are sampled closer to the initial state $\mathbf{s}_{m,0}^{(i)}$ ($a = 0$) or to the recent state $\mathbf{s}_{m,t-1}^{(i)}$ ($a = 1$), and $\mathbf{u}_t$ is a normally distributed random vector $\mathbf{u}_t \sim \mathcal{N}(0, \text{diag}[\sigma^2, \sigma^2, \sigma_\theta^2])$. In our experiments, employing more complex models (linear or accelerated motion) did not improve the performance of our method.

Further Improvements. In order to impose the some physical properties of the myocardium (expansion and shrinkage only up to some extent), we further constrain the possible state transitions and explicitly model the interaction between tags using a Markov random field (MRF) [13] with respect to the described neighborhood systems, where the additional penalty term is imposed during the weight computation in (4) if neighboring tag locations are either too close or too far from each other. The problem of possible mixing up of the particles from two neighboring tags during the prediction and update steps is solved using a deterministic spatial reclustering procedure (see more on that in [13, 14]). Additionally, the accuracy of the PF procedure is improved by using the smoothing distribution $p(\mathbf{s}_t|\mathbf{z}_{1:T})$, which combines two filtering distributions $p(\mathbf{s}_t|\mathbf{z}_{1:t})$ and $p(\mathbf{s}_{t+1}|\mathbf{z}_{t+1:T})$. The latter pdf is obtained by backward processing of the image sequence from the same initial states $\hat{\mathbf{s}}_0$, which is allowed due to the periodicity of the image sequence with the period T.

Strain Measurements. The concise description of the regional cardiac kinematics usually is given by the tensor of deformation gradients $\mathbf{T}$, which contains information of both local stretch and local twist and can be decomposed into a rigid rotation, specified by the orthogonal tensor $\mathbf{R}$, and into a pure deformation specified by the positive symmetric stretch tensor $\mathbf{D}$, as $\mathbf{T} = \mathbf{RD}$. In practice, the eigenvalues of $\mathbf{D}$, which are related to the local lengthening or shortening of the myocardial regions along the associated eigenvectors, are studied. Similar to other approaches [2–7], the tag displacements obtained by the proposed method represent the motion rather sparsely. In order to reconstruct a dense displacement field from which strain, torsion and other mechanical indices of function can be computed at all myocardial points, we used thin-plate spline interpolation [10], which is frequently used for such purpose [3, 7].

3. EXPERIMENTAL RESULTS

In-Vivo Imaging. The imaging was done using the in-house clinical 3T MRI scanner (GE Medical Systems). A SPAMM pulse sequence was used to acquire image data in experiments on healthy and diseased rats and pigs. Multiple short-axis view images of size 256×256 were collected using the following imaging parameters (rat-related, pig-related): repetition time (13, 4) msec, echo time (4, 1.25) msec, flip angle (7, 11) degrees, slice thickness (1.6, 6) mm, spacing between slices (1.6, 12) mm, pixel size (0.19×0.19, 1.25×1.25) mm^2, frames per heart cycle (24, 20), number of slice positions (7, 4), tag spacing (1.5, 6) mm, $\theta_T = 45°$.

Results. Five image sequences of rat data and five image sequences of pig data (see example images in Fig. 3 and Fig. 1, respectively) were analyzed using the proposed method. The endocardial and epicardial contours were manually drawn only in the first frame. The algorithm parameters were manually adjusted to obtain the best performance and fixed to the following values: $\sigma = 0.7$, $\sigma_\theta = 0.1$, $\gamma = 1$, $h = 1$, $a = 0.8$, $N_s = 500$. The results of tag tracking in one of such image sequences are shown in Figs. 3 and 4. According to visual

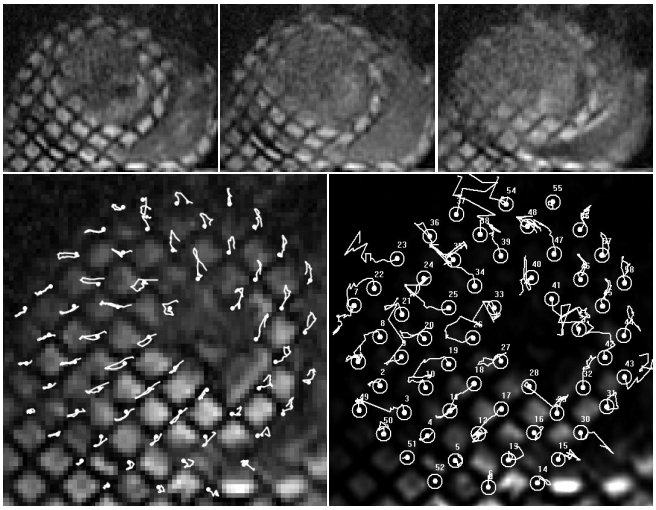


Fig. 3. Top row: examples of images from studies of rat hearts, with frames 6, 12 and 18 (out of 24 per heart cycle) showing the fading of the tagging (Courtesy P. Wielopolski, Erasmus MC). Bottom row: tag trajectories obtained using the proposed technique and Diagnosoft®HARP™.

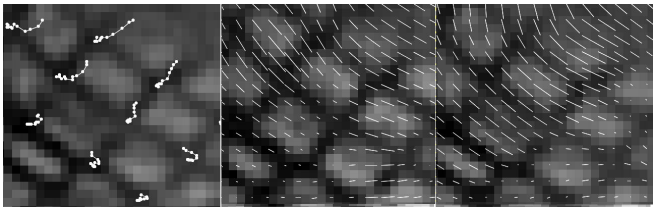


Fig. 4. Examples of strain estimation using the tracking results obtained by our algorithm and thin-plate splines for computing the eigenvalues of the strain tensor and the corresponding eigenvectors (white dashes) in two subsequent frames.

inspection, the proposed method correctly estimated the tag intersections within myocardium through the whole image sequence. The reconstructed displacement and maximal strain fields are shown in Fig. 4. Contrary to our technique, the commercially available Diagnosoft®HARP™ software for MR image analysis, frequently used for diagnosis of cardiovascular diseases, could not cope with the poor image quality and produced many erroneous tracks; reliable tag tracking was achieved only in the first 3–6 frames of the image sequence, were the tags had not faded away yet (Fig. 3).

Our PF-based algorithm was implemented in the Java programming language (Sun Microsystems Inc.) as a plugin for ImageJ (National Institutes of Health, Bethesda, MD). Tracking of 80-100 tags in a typical images sequence of 20–24 frames on a regular PC (Core 2 Duo with 2.66 GHz CPU and 3 GB of RAM) takes about 15–20 sec.

4. CONCLUSIONS

We have proposed a novel PF-based method for analysis of myocardial displacement and strain using tagged MRI. The method is built within a Bayesian estimation framework and incorporates prior knowledge about the tag dynamics and appearance, which makes it robust against typically poor image quality and intrinsic tag fading. Experiments on two types of real (small) animal imaging data and comparison with commercially available software confirmed that the method is capable of accurate displacement and strain estimation with minimal user interaction and can be used in practice for fast data analysis. Our future work will address the question of probabilistic LV contour detection and fusion of two approaches into one fully automatic PF-based method that will be extensively validated and used in our further studies for classification of healthy and diseased heart dynamics.

5. REFERENCES

[1] L. Axel and L. Dougherty, "MR imaging of motion with spatial modulation of magnetization," *Radiology*, vol. 171, pp. 841–845, 1989.

[2] A. A. Young, D. L. Kraitchman, L. Dougherty, and L. Axel, "Tracking and finite element analysis of stripe deformation in magnetic resonance tagging," *IEEE Transactions on Medical Imaging*, vol. 14, no. 3, pp. 413–421, 1995.

[3] S. Kumar and D. Goldgof, "Automatic tracking of SPAMM grid and the estimation of deformation parameters from cardiac MR images," *IEEE Transactions on Medical Imaging*, vol. 13, no. 1, pp. 122–132, 1994.

[4] D. L. Kraitchman, A. A. Young, Ch.-N. Chang, and L. Axel, "Semi-automatic tracking of myocardial motion in MR tagged images," *IEEE Transactions on Medical Imaging*, vol. 14, no. 3, pp. 422–433, 1995.

[5] M. A. Guttman, J. L. Prince, and E. R. McVeigh, "Tag and contour detection in tagged MR images of the left ventricle," *IEEE Transactions on Medical Imaging*, vol. 13, no. 1, pp. 74–88, 1994.

[6] X. Deng and T. S. Denney, Jr., "Three-dimensional myocardial strain reconstruction from tagged MRI using a cylindrical B-spline model," *IEEE Transactions on Medical Imaging*, vol. 23, no. 7, pp. 861–867, 2004.

[7] A. A. Amini, Yasheng Chen, R. W. Curwen, V. Mani, and J. Sun, "Coupled B-snake grids and constrained thin-plate splines for analysis of 2-D tissue deformations from tagged MRI," *IEEE Transactions on Medical Imaging*, vol. 17, no. 3, pp. 344–356, 1998.

[8] N. F. Osman, E. R. McVeigh, and J. L. Prince, "Imaging heart motion using harmonic phase MRI," *IEEE Transactions on Medical Imaging*, vol. 19, no. 3, pp. 186–202, 2000.

[9] T. S. Denney, Jr. and J. L. Prince, "Reconstruction of 3-D left ventricular motion from planar tagged cardiac MR images: an estimation theoretic approach," *IEEE Transactions on Medical Imaging*, vol. 14, no. 4, pp. 625–635, 1995.

[10] F. L. Bookstein, "Principal warps: Thin-plate splines and the decomposition of deformations," *IEEE Transactions on Pattern Analysis and Machine Intelligence*, vol. 11, no. 6, pp. 567–585, 1989.

[11] S. M. Arulampalam, S. Maskell, N. Gordon, and T. Clapp, "A tutorial on particle filters for online nonlinear/non-Gaussian Bayesian tracking," *IEEE Transactions on Signal Processing*, vol. 50, no. 2, pp. 174–188, 2002.

[12] A. Doucet, N. de Freitas, and N. Gordon, *Sequential Monte Carlo Methods in Practice*, Springer-Verlag, Berlin, 2001.

[13] I. Smal, K. Draegestein, N. Galjart, W. Niessen, and E. Meijering, "Particle filtering for multiple object tracking in dynamic fluorescence microscopy images: Application to microtubule growth analysis," *IEEE Transactions on Medical Imaging*, vol. 27, no. 6, pp. 789–804, 2008.

[14] J. Vermaak, A. Doucet, and P. Pérez, "Maintaining multi-modality through mixture tracking," in *Proceedings of the IEEE International Conference on Computer Vision*, 2003, pp. 1110–1116.